

Testing shape selection in directional solidification

John Bechhoefer and Albert Libchaber

The James Franck and Enrico Fermi Institutes, The University of Chicago, Chicago, Illinois 60637

(Received 26 September 1986)

We report results from an experiment on the directional solidification of pivalic acid. In addition to the usual cellular interface patterns, we observe a new, metastable dendritic form that can be interpreted in the light of recent ideas about pattern formation.

When a thin layer of pivalic acid is drawn at a fixed velocity across a linear temperature gradient, the solid-liquid interface between crystalline pivalic acid and its melt assumes a cellular pattern. Deep liquid grooves separate periodically spaced fingers of solid. Although such patterns are familiar from previous experiments on other materials,¹ the cells in pivalic acid are unusual in that the tips of the patterns are stable and do not split, except at very low solidification velocities. We believe that this behavior is related to the large amount of surface-tension anisotropy in pivalic acid.² In the experiments reported below, we have taken advantage of this stability to probe patterns close to those naturally selected by the system, thereby testing recent theories concerning the mechanism of pattern formation.

In a directional solidification experiment, if we start from rest and switch on a given velocity, the system eventually selects a well-defined, stable cell wavelength that is a function of the velocity. If we start with one velocity, allow a wavelength to be selected, and then change the solidification velocity, the selected wavelength will in general also change. If the new wavelength is smaller than the old, the usual way to reduce the cell size is through tip splitting. But in pivalic acid, tip splitting is inhibited; instead, we observe hysteresis. (See Fig. 1.) When we increase the velocity, the tips sharpen and give rise to time-dependent sidebranches. Alternatively, forcibly changing the wavelength while fixing the velocity also leads to time-dependent patterns. Thus, small perturbations in the shape of a smooth, time-independent cell lead to a time-dependent metastable shape that can exist for arbitrarily long times.

Our experiment follows Jackson's design for his original work on directional solidification.³ A thin glass cell containing pivalic acid is placed atop two temperature-controlled copper blocks that are separated by a small gap. One block is kept hotter than the melting temperature of pivalic acid, the other cooler, so that there is a solid-liquid interface that sits over the gap between the two plates. The sample cell is then drawn at a constant velocity v across the gap, from the hot to the cold side. After a sometimes slow transient, the solid-liquid interface will move with a velocity $-v$ so that its average position is maintained at a constant temperature.

In the experiments reported here, the hot block was electrically heated to 55.0°C and regulated to $\pm 0.1^\circ\text{C}$. The cold block was cooled to $10.0^\circ\text{C} \pm 0.1^\circ\text{C}$ by circulat-

ing water through it. The gap between the two blocks was 0.200 ± 0.001 cm. The temperature gradient varied considerably as a function of the thickness of the sample plates and the solidification velocities and was calibrated by building a dummy cell with a thermocouple. For low velocities, the gradient was approximately $125^\circ\text{C}/\text{cm}$, and it rose for higher velocities. The sample was pushed by a stepping-motor lead-screw combination at velocities that ranged from $0.5 \mu\text{m}/\text{sec}$ to $260 \mu\text{m}/\text{sec}$. The sample cell was constructed from two 22-mm-square number one microscope cover glass slips glued all around, except for entrance and exit holes. Stycast, once hardened, proved to be a relatively inert glue. The cell had a thickness of approximately $20 \mu\text{m}$ and was filled with pivalic acid under vacuum. The fill holes were sealed with epoxy.

From 6°C to 36.5°C , pivalic acid forms a soft fcc crystal that is known as a plastic crystal phase. It is thus very similar to succinonitrile and carbon tetrabromide, which have been used in previous directional solidification experiments. Pivalic acid differs markedly from other plastic crystals in its large surface tension anisotropy. Glicksman has recently measured the relative anisotropy ϵ to be 5%, in contrast to 0.5% for succinonitrile.⁴ ϵ is defined via the relation $\gamma = \gamma_0 \{1 + \epsilon [1 - \cos(4\theta)]\}$, where γ_0 is the

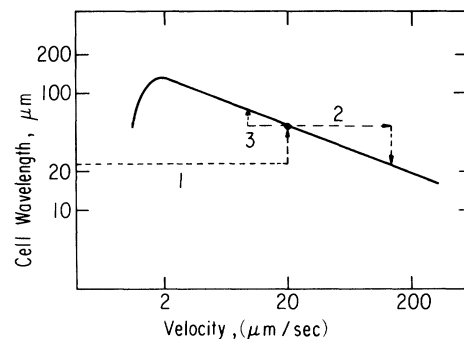


FIG. 1. Cell wavelength vs velocity for pivalic acid. The selected velocity was observed by starting from rest (line 1). Line 2 shows the hysteresis observed as the velocity is increased. The wavelength collapses when the solidification velocity is about eight times the initial velocity. Line 3 shows the smaller amount of hysteresis observed as the velocity is decreased. The system begins to choke off cells once the velocity is about half its initial value.

surface tension in the $\langle 100 \rangle$ direction and θ is the angle between the orientation of the surface and the $\langle 100 \rangle$ direction.

Previous experiments in succinonitrile have shown three types of interface shapes.⁴ Below a critical velocity v_c , the interface is flat. Linear stability analysis predicts that $v_c = DGk / [|dT/dC| C_0(1-k)]$, where D is the diffusion coefficient of impurities in the liquid, G is the temperature gradient, C_0 is the average concentration of impurities, dT/dC is the liquidus slope, and k is the partition coefficient. Between v_c and about $10v_c$, solid fingers freeze with impurity-rich, liquid grooves in between. The wavelength of the cells increases with velocity, while the tip curvature decreases. Above about $10v_c$, the cellular patterns develop sidebranches and become dendritic. In this regime, both the wavelength and tip curvature decrease with velocity.

Our sample of pivalic acid was distilled twice under vacuum. For the impurities, we measured $D \approx 10^{-6}$ cm²/sec (Ref. 2). This value of D is a factor of 10 smaller than that reported for succinonitrile and acetone⁶ but is consistent with other data obtained from our experiment. We also measured $(dT/dC)C_0$ to be 2.9°C.

In pivalic acid, we observed a cellular solid-liquid interface over the entire 500-fold speed range of our driving motor. The dependence of wavelength on velocity is similar to that of succinonitrile—for $v_c < v < 10v_c$, it increases; for $v > 10v_c$, it decreases—but the shape is always cellular. Also, for $v < 10v_c$, the diffusion length D/v is larger than the cell wavelength; for $v > 10v_c$, it is smaller. We have good reason to suspect that the greatly expanded cellular regime is due to the high crystalline anisotropy of pivalic acid.² What is important for this study is first that there is a wide range of velocities over which one finds very stable cells. Second, the wavelength of cells of pivalic acid increases at low velocities (in our experiment, below 2 $\mu\text{m}/\text{sec}$) and decreases at higher velocities, following approximately the same laws that govern the length scales of cells and dendrites of succinonitrile. Third, and most important, where the wavelength of cells decreases with velocity, the tips of the cells were absolutely stable and were never observed to split.

The solid part of our sample was a single crystal whose $\langle 100 \rangle$ direction was aligned with the thermal gradient. When the crystallographic axes are not so aligned, the fingers grow at an angle to the thermal gradient, as described previously.⁷

In our experiments, we started from rest and switched on a given velocity. After the system had evolved to a stable system of cells, we increased the velocity. Figure 2(a) shows stationary cells 10 $\mu\text{m}/\text{sec}$. The velocity is then doubled successively in Figs. 2(b), 2(c), and 2(d). The overall size of the cell is fixed by the initial conditions, and the shape that is observed has the same wavelength as the original cells. The solution, however, is no longer stationary, for in the frame in which the tip of the dendrites is fixed, the sidebranches advect to the rear.

Figure 2 shows that the wavelength remains fixed as the velocity is increased eight fold. As the velocity is further increased, the sidebranches will themselves sprout sidebranches. Note that the system remains dendritic,

even after the wavelength has decreased. The wavelength after collapse is still 50 to 100% larger than the selected wavelength. This collapse of metastable dendrites is shown in Fig. 3.

Figure 2 also reveals that the tip is sharpening up as the velocity is increased. Because the tip is the "farthest out" part of the cell, its curvature depends only on *local* conditions (velocity, temperature gradient, etc.) and not on the global structure of the fingers, as determined by initial conditions. To test this hypothesis, we made another series of runs where we started from different initial conditions and increased the velocity to the same final value.

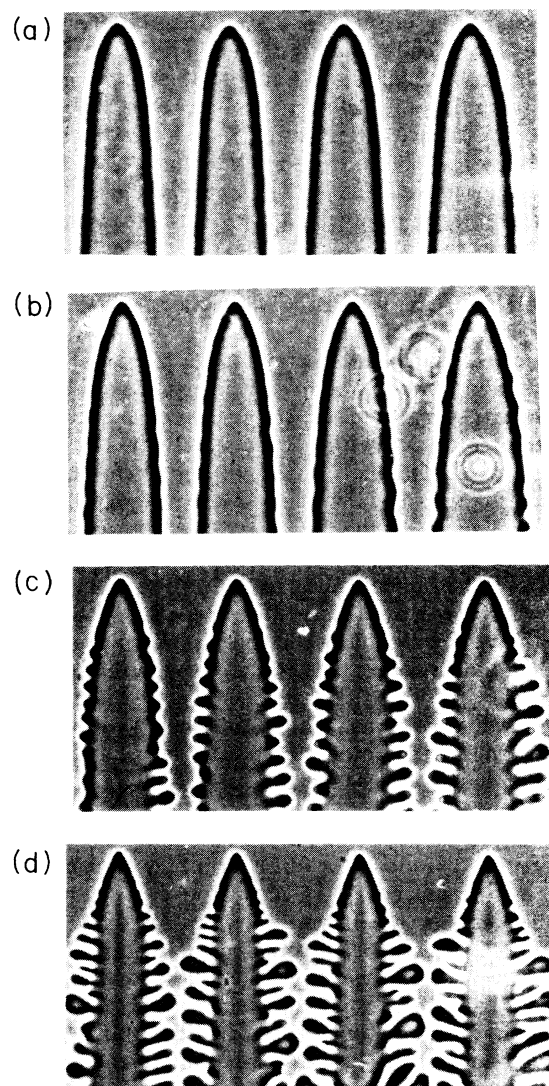


FIG. 2. Constant wavelength, variable tip curvature. (a) shows the initial condition: stable cells solidifying at 10 $\mu\text{m}/\text{sec}$. (b) shows the same sample after the velocity has been increased to 20 $\mu\text{m}/\text{sec}$. In (c), the velocity is 40 $\mu\text{m}/\text{sec}$ and (d), it is 80 $\mu\text{m}/\text{sec}$. All of the pictures reflect steady state conditions. The cell wavelength is 75 μm .

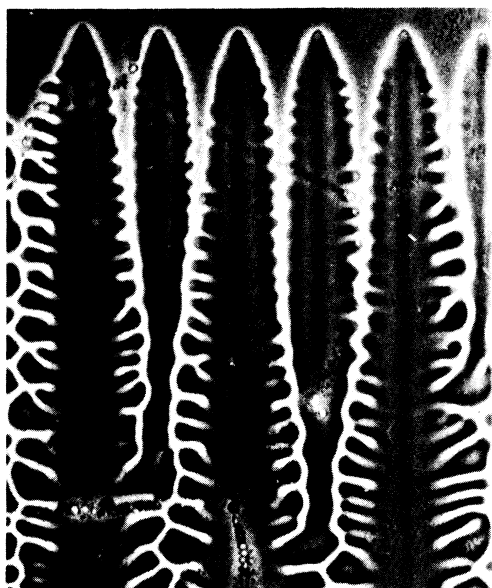


FIG. 3. Collapsing dendrites. The initial velocity was $5 \mu\text{m}/\text{sec}$. That shown is $40 \mu\text{m}/\text{sec}$. At $5 \mu\text{m}/\text{sec}$, the wavelength was $107 \mu\text{m}$; at $40 \mu\text{m}/\text{sec}$, the wavelength is $45 \mu\text{m}$.

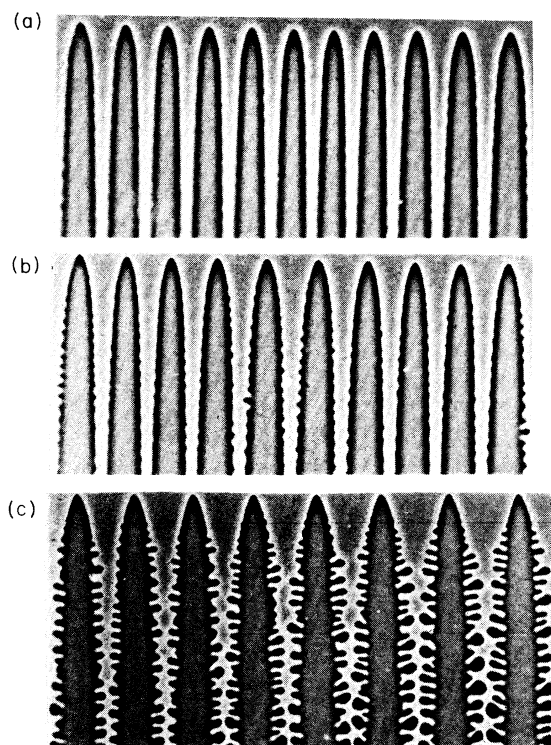


FIG. 4. Constant tip curvature, variable wavelength. The solidification rate is $40 \mu\text{m}/\text{sec}$ for all photos. In (a), the initial velocity is also $40 \mu\text{m}/\text{sec}$ (after starting from rest). In (b), the initial velocity was $30 \mu\text{m}/\text{sec}$, and in (d) it was $15 \mu\text{m}/\text{sec}$.

Figure 4 shows one stable cell at $40 \mu\text{m}/\text{sec}$. Figure 4(b) shows a dendrite at $40 \mu\text{m}/\text{sec}$ that came from a stable cell at $30 \mu\text{m}/\text{sec}$, and so forth. Although the differing initial conditions lead to differing wavelengths for each of the fingers, each one has the same tip curvature, as expected.

Finally, Fig. 5 shows the result of starting from a high velocity and reducing it. The wavelength of the cells increases by a "choking off" mechanism. One cell lags slightly and then is choked off by its two neighbors. It is because the choking off mechanism operates in pivalic acid that one is able to observe the selected wavelength. When a flat interface destabilizes, the initial wavelength is always two or four times smaller than the selected cell size. The selection always goes from smaller to larger wavelengths and can thus be observed in pivalic acid.

To summarize, we have independently changed the tip curvature $1/\rho$ and the wavelength λ , only one combination of which, for a given velocity, gives time-independent patterns. Thus, the stationary cellular shape of directional

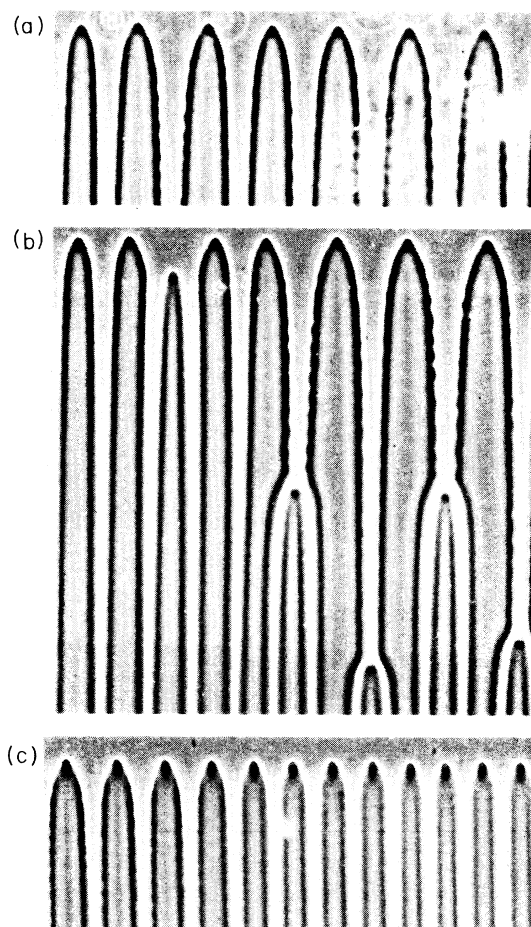


FIG. 5. Choking off mechanism. (c) shows cells at $80 \mu\text{m}/\text{sec}$. (b) shows the choking off process that occurs when the velocity is abruptly reduced to $40 \mu\text{m}/\text{sec}$. (a) shows the final state at $40 \mu\text{m}/\text{sec}$. At $80 \mu\text{m}/\text{sec}$, the wavelength was $87 \mu\text{m}$, while at $40 \mu\text{m}/\text{sec}$, it was $144 \mu\text{m}$.

solidification is an isolated solution in the space of nearby shapes. By forcibly changing the shape at the tip or at the far end, we immediately observe time-dependent patterns. We are currently studying the dependence of the wavelength and growth rate of the sidebranches on the mismatch and the velocity.

These observations are relevant to recent theories of pattern selection in diffusive processes. In the absence of surface tension, such processes generally admit a continuous family of stationary solutions; however, only one shape is observed in experiments. If we look only for stationary solutions, the theory of "microscopic solvability" predicts that the introduction of surface tension along the moving interface will break up the continuous family into a discrete, countably infinite set of solutions. The theory has been applied to numerical analysis of the Saffman-Taylor problem of viscous fingering in fluids,^{8,9} dendritic crystal growth into an undercooled melt,^{6,10,11} and direc-

tional solidification.¹² It has also been used to solve the Saffman-Taylor fingerselection problem analytically.¹³⁻¹⁶

Our observation that the cellular shape is an isolated solution in the space of nearby shapes thus agrees with a prediction of microscopic solvability. We are currently looking for the other solutions.

Finally, if the slight irregularities in the sidebranches are ignored, then the metastable dendrites in Figs. 2 and 4 would be periodic solutions. A natural question to ask then is "Does a slight mismatch in the microscopic solvability condition lead to a periodic solution?" If so, then the qualitative test of microscopic solvability presented here can be made quantitative.

This work was supported by the National Science Foundation, under Grant No. NSF DMR83-16204. One of us (J.B.) received support from AT&T Bell Labs.

¹J. S. Langer, *Rev. Mod. Phys.* **52**, 1 (1980).

²K. A. Jackson and J. D. Hunt, *Acta. Metal.* **13**, 1212 (1965).

³M. Glicksman, *Mat. Sci. Eng.* **65**, 45 (1984).

⁴R. Trivedi, *Metal. Trans.* **15A**, 977 (1984). Cf. W. Kurz and D. J. Fisher, *Acta Metal.* **29**, 11 (1981); and H. Esaka, Ph.D. thesis, Ecole Polytechnique Federale de Lausanne, 1986.

⁵J. Bechhoefer and A. Libchaber (unpublished).

⁶M. Glicksman, R. Schaeffer, and J. D. Ayers, *Metal. Trans.* **7A**, 1747 (1976).

⁷F. Heslot and A. Libchaber, *Phys. Scr.* **T9**, 126 (1985).

⁸P. G. Saffman and G. I. Taylor, *Proc. R. Soc. London, Ser. A*

245, 312 (1958).

⁹J.-M. Vanden-Broeck, *Phys. Fluids* **26**, 2033 (1983).

¹⁰D. Meiron, *Phys. Rev. A* **33**, 2704 (1986).

¹¹D. Kessler, J. Koplik, and H. Levine, *Phys. Rev. A* **33**, 3352 (1986).

¹²A. Karma, *Phys. Rev. A* **34**, 4353 (1986).

¹³B. Shraiman, *Phys. Rev. Lett.* **56**, 2028 (1986).

¹⁴D. C. Hong and J. S. Langer, *Phys. Rev. Lett.* **56**, 2032 (1986).

¹⁵R. Combescot, T. Dombre, V. Hakim, Y. Pomeau, and A. Pumir, *Phys. Rev. Lett.* **56**, 2036 (1986).

¹⁶M. D. Kruskal and H. Segur (unpublished).

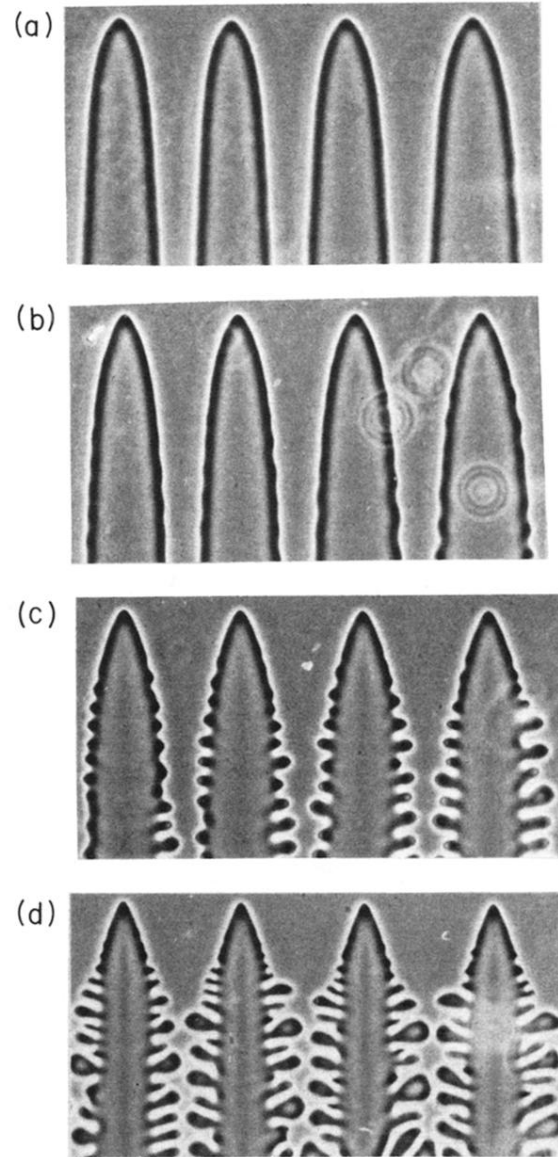


FIG. 2. Constant wavelength, variable tip curvature. (a) shows the initial condition: stable cells solidifying at $10 \mu\text{m}/\text{sec}$. (b) shows the same sample after the velocity has been increased to $20 \mu\text{m}/\text{sec}$. In (c), the velocity is $40 \mu\text{m}/\text{sec}$ and (d), it is $80 \mu\text{m}/\text{sec}$. All of the pictures reflect steady state conditions. The cell wavelength is $75 \mu\text{m}$.

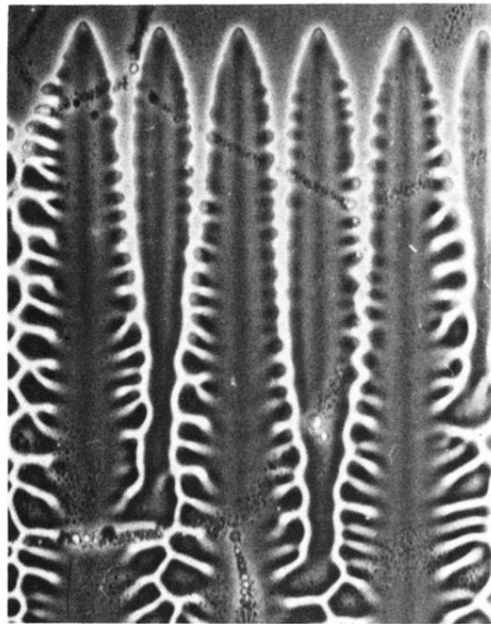


FIG. 3. Collapsing dendrites. The initial velocity was $5 \mu\text{m}/\text{sec}$. That shown is $40 \mu\text{m}/\text{sec}$. At $5 \mu\text{m}/\text{sec}$, the wavelength was $107 \mu\text{m}$; at $40 \mu\text{m}/\text{sec}$, the wavelength is $45 \mu\text{m}$.

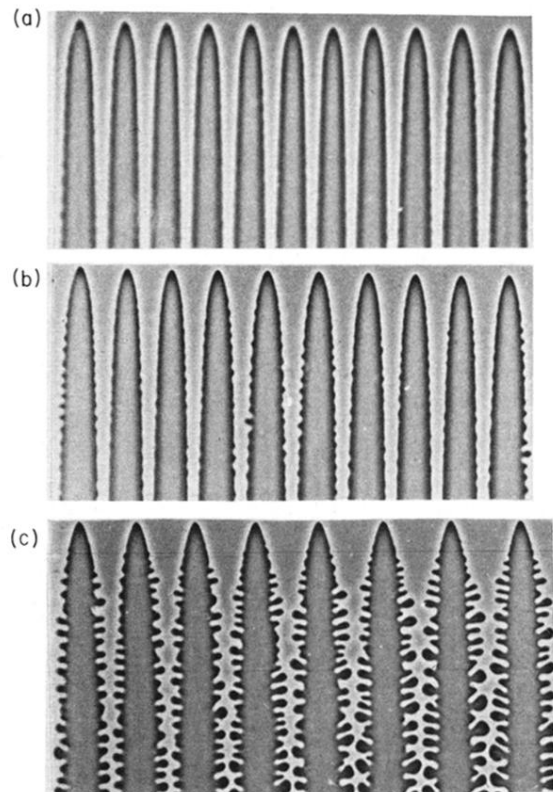


FIG. 4. Constant tip curvature, variable wavelength. The solidification rate is $40 \mu\text{m}/\text{sec}$ for all photos. In (a), the initial velocity is also $40 \mu\text{m}/\text{sec}$ (after starting from rest). In (b), the initial velocity was $30 \mu\text{m}/\text{sec}$, and in (d) it was $15 \mu\text{m}/\text{sec}$.

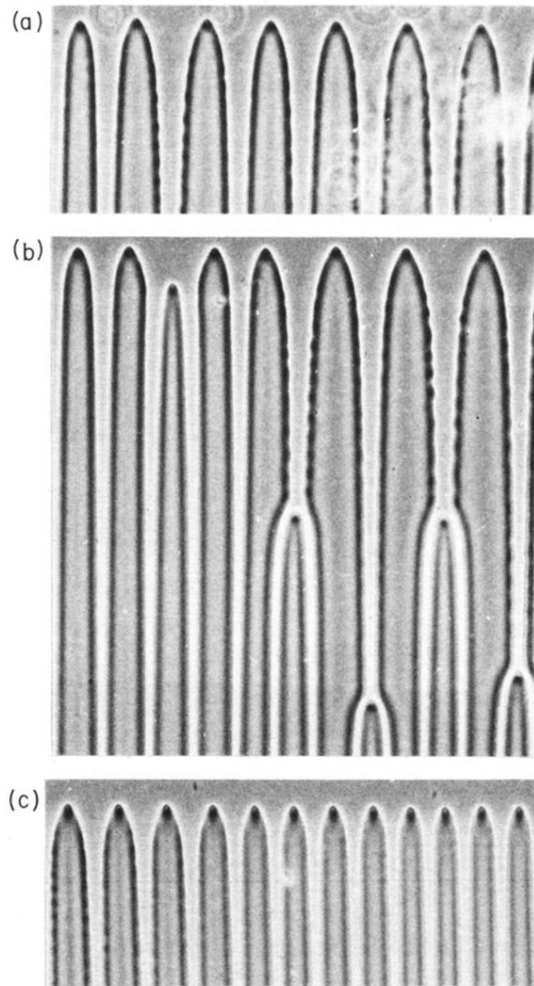


FIG. 5. Choking off mechanism. (c) shows cells at 80 $\mu\text{m}/\text{sec}$. (b) shows the choking off process that occurs when the velocity is abruptly reduced to 40 $\mu\text{m}/\text{sec}$. (a) shows the final state at 40 $\mu\text{m}/\text{sec}$. At 80 $\mu\text{m}/\text{sec}$, the wavelength was 87 μm , while at 40 $\mu\text{m}/\text{sec}$, it was 144 μm .